

DET NORSKE VERITAS

**Classification and
Registry of Shipping**

Publication No. 90 – Sept. 1975

MOTIONS OF LARGE STRUCTURES IN WAVES AT ZERO FROUDE NUMBERS

O.M. Faltinsen and F.C. Michelsen

Motions of Large Structures in Waves at Zero Froude Number^o

O. M. Faltinsen* F. C. Michelsen†

1 INTRODUCTION

The offshore activities in the North Sea have resulted in many offshore structures that are rather large in volume and not amenable to two-dimensional analysis. As examples may be mentioned the 'Ekofisk' oil storage tank and the 'Condeep' platform. For those large volume three-dimensional forms one cannot rely on the Morison-type equation (Morison *et al.* (1))‡ or strip theory to calculate hydrodynamic wave forces and moments. One has to resort to numerical schemes based on three-dimensional source techniques or the use of Green's theorem. This has been done by Lebreton and Cormault (2), Garrison and Seetharama Rao (3), Milgram and Halkyard (4) and van Oortmersen (5).

In this paper the source technique has been applied to a floating object in regular waves and the added mass and damping coefficients, the wave exciting force and moment and the motions in six degrees of freedom and the pressure distribution have been calculated. The horizontal drift force and moment have also been evaluated.

Notation

(Additional nomenclature used in the Appendices are defined only as they appear.)

A_{jk}	Added-mass coefficients ($j, k = 1, 6$).
A_{wp}	Area of water plane.
B_{jk}	Damping coefficients.
C_{jk}	Restoring coefficients.
ds	Element of area.
$F(\theta)$	See equation (37)
$F_j e^{-i\omega t}$	Exciting force and moment components ($j = 1, 6$).
G	Green's function. See equations (23) and (24)
g	Gravitational acceleration.
h	Water depth.
I_j	Moment of inertia in j th mode.
I_{jk}	Product of inertia.
i	$\sqrt{-1}$.
J_0	Bessel function of first kind of zero order.
K_0	Modified Bessel function of second kind of zero order.
k	Wave number.
M	Mass of the body.
n	Unit normal into the fluid.
n_i	See equations (19) and (20); $i = 1, 6$
n_j	Displacements, ($j = 1, 2, \dots, 6$ refer to surge, sway, heave, roll, pitch and yaw, respectively; see Fig. 1).
Q_j	Source densities, $j = 1, 7$. See equation (22)

The MS. of this paper was accepted for publication on 5th February 1974.

* Senior Research Engineer, Det norske Veritas, Postboks 6060, Etterstad, Oslo 6, Norway.

† Professor, The Technical University of Norway, Trondheim, Norway.

‡ References are given in Appendix 4.

R	$= \sqrt{[(x - \xi)^2 + (y - \eta)^2 + (z - \zeta)^2]}$
R^1	$= \sqrt{[(x - \xi)^2 + (y - \eta)^2 + (z + 2h + \zeta)^2]}$
r, θ, z	Cylindrical polar co-ordinates with $x = r \cos \theta$ and $y = r \sin \theta$.
r_1	$= \sqrt{[(x - \xi)^2 + (y - \eta)^2]}$
r	Position vector.
S	Average wetted surface of the body.
S_∞	Vertical circular cylinder of large radius.
t	Time variable.
V	Displaced volume of water.
V_r, V_θ, V_z	Fluid velocity components in cylindrical polar co-ordinate system.
x, y, z	Co-ordinate system as defined in Fig. 1.
Y_0	Bessel function of second kind of zero order.
Z_B	z -co-ordinate of centre of buoyancy.
Z_G	z -co-ordinate of centre of gravity.
β	Direction of propagation of incident waves ($\beta = 0$ means propagation along the positive x -axis).
ζ_a	Wave amplitude of incident waves.
λ	Wavelength.
v	$= (\omega^2/g) = k \tanh kh$.
ξ, η, ζ	Co-ordinates of a point on the surface of the object.
ρ	Mass density of water.
$\phi(\theta)$	See equation (37)
ϕ	Velocity potential.
ϕ_j	See equation (11), $j = 0, 7$
ω	Circular frequency of wave.

2 THE EQUATIONS OF MOTION

A right-handed co-ordinate system (x, y, z) fixed with respect to the mean position of the body is used, with positive z vertically upwards through the centre of gravity of the body and the origin in the plane of the undisturbed free surface. The body is assumed to have the x - z plane as a plane of symmetry. Let the translatory displacements in the x, y and z directions with respect to the origin be η_1, η_2 and η_3 respectively, so that η_1 is the surge, η_2 is the sway and η_3 is the heave displacement. Furthermore, let the angular displacement of the rotational motion about the x, y and z axes be η_4, η_5 and η_6 , respectively, so that η_4 is the roll, η_5 is the pitch and η_6 is the yaw angle. The co-ordinate system and the translatory and angular displacements conventions are shown for the case of a ship in Fig. 1.

The linear frequency domain equations of motion in regular incident waves of small amplitude can for a body symmetric with respect to the x - z plane and under the assumption that responses are linear and harmonic be written as follows:

$$(M + A_{11})\ddot{\eta}_1 + B_{11}\dot{\eta}_1 + A_{13}\ddot{\eta}_3 + B_{13}\dot{\eta}_3 + (MZ_G + A_{15})\ddot{\eta}_5 + B_{15}\dot{\eta}_5 = F_1 e^{-i\omega t} \dots (1)$$

$$A_{31}\ddot{\eta}_1 + B_{31}\dot{\eta}_1 + (M + A_{33})\ddot{\eta}_3 + B_{33}\dot{\eta}_3 + C_{33}\eta_3 + A_{35}\ddot{\eta}_5 + B_{35}\dot{\eta}_5 + C_{35}\eta_5 = F_3 e^{-i\omega t} \quad \dots(2)$$

$$(MZ_G + A_{51})\ddot{\eta}_1 + B_{51}\dot{\eta}_1 + A_{53}\ddot{\eta}_3 + B_{53}\dot{\eta}_3 + C_{53}\eta_3 + (I_5 + A_{55})\ddot{\eta}_5 + B_{55}\dot{\eta}_5 + C_{55}\eta_5 = F_5 e^{-i\omega t} \quad \dots(3)$$

$$(M + A_{22})\ddot{\eta}_2 + B_{22}\dot{\eta}_2 + (A_{24} - MZ_G)\ddot{\eta}_4 + B_{24}\dot{\eta}_4 + A_{26}\ddot{\eta}_6 + B_{26}\dot{\eta}_6 = F_2 e^{-i\omega t} \quad \dots(4)$$

$$(A_{42} - MZ_G)\ddot{\eta}_2 + B_{42}\dot{\eta}_2 + (A_{44} + I_4)\ddot{\eta}_4 + B_{44}\dot{\eta}_4 + C_{44}\eta_4 + (A_{46} - I_{46})\ddot{\eta}_6 + B_{46}\dot{\eta}_6 = F_4 e^{-i\omega t} \quad \dots(5)$$

$$A_{62}\ddot{\eta}_2 + B_{62}\dot{\eta}_2 + (A_{64} - I_{46})\ddot{\eta}_4 + B_{64}\dot{\eta}_4 + (A_{66} + I_6)\ddot{\eta}_6 + B_{66}\dot{\eta}_6 = F_6 e^{-i\omega t} \quad \dots(6)$$

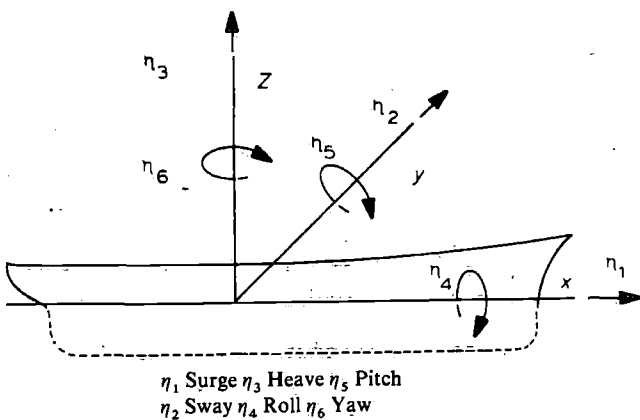


Fig. 1. Sign convention for translatory and angular displacements

Here M is the mass of the body, I_j the moment of inertia and I_{jk} the product of inertia. The inertia terms are with respect to the co-ordinate system shown in Fig. 1. Further Z_G is the z -co-ordinate of the centre of gravity. A_{jk} and B_{jk} are the added-mass and damping coefficients and F_j are the complex amplitudes of the wave exciting force and moment, with the force and moment given by the real part of $F_j e^{-i\omega t}$ (It is understood that real part is to be taken in expressions involving $e^{-i\omega t}$). F_1, F_2 and F_3 refer to the amplitudes of the surge, sway and heave exciting forces, while F_4, F_5 and F_6 are the amplitudes of the roll, pitch and yaw exciting moments; ω is the frequency of the waves and is the same as the frequency of the response. The dots stand for time derivatives so that $\dot{\eta}_k$ and $\ddot{\eta}_k$ are velocity and acceleration terms.

The body is free-floating so the restoring coefficients follow from hydrostatic and mass considerations. They are given by

$$C_{33} = \rho g A_{wp} \quad \dots(7)$$

$$C_{35} = C_{53} = -\rho g \iint_{A_{wp}} x ds \quad \dots(8)$$

$$C_{44} = \rho g V (Z_B - Z_G) + \rho g \iint_{A_{wp}} y^2 ds \quad \dots(9)$$

$$C_{55} = \rho g V (Z_B - Z_G) + \rho g \iint_{A_{wp}} x^2 ds \quad \dots(10)$$

Here ρ is the mass density of the water, g is the gravita-

tional acceleration. A_{wp} is the water plane area, V is the displaced volume of water and Z_B is the z co-ordinate of the centre of buoyancy. The integration is over the water plane area.

The added-mass and damping coefficients and the exciting force and moment are derived in the next Section.

3 THE HYDRODYNAMIC BOUNDARY-VALUE PROBLEM

Viscous effects are neglected and we assume the fluid to be incompressible. The depth h is finite and constant and the free surface is infinite in all directions. The motion of the body and the fluid is assumed to be small so that we can linearize the body boundary condition and the free surface condition.

The problem can be formulated in terms of potential flow theory. We assume that steady-state conditions have been obtained and write the total velocity potential as:

$$\phi = \phi_0 e^{-i\omega t} + \phi_7 e^{-i\omega t} + \sum_{i=1}^6 \phi_i \dot{\eta}_i \quad \dots(11)$$

where $\phi_0 e^{-i\omega t}$ is the velocity potential of the incident waves, which can be written as

$$\phi_0 e^{-i\omega t} = \frac{g\zeta_a}{\omega} \frac{\cosh k(z+h)}{\cosh kh} e^{i(kx \cos \beta + ky \sin \beta - \omega t)} \quad \dots(12)$$

Here ζ_a is the wave amplitude and β the direction of propagation of incident waves. k is the wave number, which is related to the frequency of the waves by the dispersion relationship

$$\frac{\omega^2}{g} = k \tanh kh \quad \dots(13)$$

Further, $\phi_7 e^{-i\omega t}$ is the diffraction potential for the restrained body and $\phi_j, j = 1, 6$, is the contribution to the velocity potential from the j th mode of motion.

It can be shown that $\phi_j, j = 0, 7$, must satisfy

$$\frac{\partial^2 \phi_j}{\partial x^2} + \frac{\partial^2 \phi_j}{\partial y^2} + \frac{\partial^2 \phi_j}{\partial z^2} = 0 \text{ in the fluid domain} \quad \dots(14)$$

$$-\omega^2 \phi_j + g \frac{\partial \phi_j}{\partial z} = 0 \text{ on } z = 0 \quad \dots(15)$$

$$\frac{\partial \phi_j}{\partial z} = 0 \text{ on } z = -h \quad \dots(16)$$

Further, $\phi_j \dot{\eta}_j, j = 1, 6$, and $\phi_7 e^{-i\omega t}$ satisfy a radiation condition and the following body boundary conditions on the average position of the wetted surface of the body

$$\frac{\partial \phi_j}{\partial n} = n_j, \quad j = 1, 6 \quad \dots(17)$$

$$\frac{\partial \phi_7}{\partial n} = -\frac{\partial \phi_0}{\partial n} \quad \dots(18)$$

Here $\partial/\partial n$ is the normal derivative in the direction of the outward normal \mathbf{n} to the surface of the body.

Further $n_j, j = 1, 6$, is defined by

$$\mathbf{n} = (n_1, n_2, n_3) \quad \dots(19)$$

and

$$\mathbf{r} \times \mathbf{n} = (n_4, n_5, n_6) \quad \dots(20)$$

where r is the position vector

$$r = xi + yj + zk \quad \dots (21)$$

It is possible to show that the solution of ϕ_j ($j = 1, 7$) can be written as

$$\phi_j = \iint_S Q_j(\xi, \eta, \zeta) G(x, y, z; \xi, \eta, \zeta) ds \quad \dots (22)$$

This has been shown by Lamb (6) for the infinite fluid case. The integration in equation (22) is over the average wetted surface S of the body with (ξ, η, ζ) being the co-ordinates of a point on S . Q_j is the unknown source density function and $G(x, y, z; \xi, \eta, \zeta)$ is the Green's function for the problem, which can be written in two ways as follows (see Weehäusen and Laitone (7)).

$$\begin{aligned} G(x, y, z; \xi, \eta, \zeta) &= \frac{2\pi(v^2 - k^2)}{k^2h - v^2h + v} \cosh k(z + h) \\ &\times \cosh k(\zeta + h) (Y_0(kr_1) - iJ_0(kr_1)) \\ &+ 4 \sum_{k=1}^{\infty} \frac{\mu_k^2 + v^2}{\mu_k^2h + v^2h - v} \cos(\mu_k(z + h)) \\ &\times \cos(\mu_k(\zeta + h)) K_0(\mu_k r_1) \quad \dots (23) \end{aligned}$$

or

$$\begin{aligned} G(x, y, z; \xi, \eta, \zeta) &= \frac{1}{R} + \frac{1}{R^1} \\ &+ 2PV \int_0^{\infty} \frac{(\mu + v) e^{-\mu h} \cosh \mu(\zeta + h) \cosh \mu(z + h) J_0(\mu r_1) d\mu}{\mu \sinh \mu h - v \cosh \mu h} \\ &+ i \frac{2\pi(k^2 - v^2) \cosh k(\zeta + h) \cosh k(z + h)}{k^2h - v^2h + v} J_0(kr_1) \quad \dots (24) \end{aligned}$$

In equation (23) μ_k is the solutions of the equation

$$\mu_k \tan \mu_k h + v = 0 \quad \dots (25)$$

J_0 is the Bessel function of the first kind of zero order; Y_0 is the Bessel function of the second kind of zero order; K_0 is the modified Bessel function of the second kind of zero order; and

$$v = \frac{\omega^2}{g} \quad \dots (26)$$

$$R = \sqrt{[(x - \xi)^2 + (y - \eta)^2 + (z - \zeta)^2]} \quad \dots (27)$$

$$R^1 = \sqrt{[(x - \xi)^2 + (y - \eta)^2 + (z + 2h + \zeta)^2]} \quad \dots (28)$$

$$r_1 = \sqrt{[(x - \xi)^2 + (y - \eta)^2]} \quad \dots (29)$$

In equation (24) PV indicates a principal value integral. For practical purposes equation (23) is used when $kr_1 \geq 0.1$ and equation (24) when $kr_1 < 0.1$. It was found convenient to rewrite equation (24). This is shown in Appendix 1.

The source densities Q_j in equation (22) are found by satisfying the body boundary conditions (17) and (18). This results in the following two-dimensional Fredholm integral equations of the second kind over the surface S

$$\begin{aligned} -2\pi Q_j(x, y, z) + \iint_S Q_j(\xi, \eta, \zeta) \frac{\partial}{\partial n} (G(x, y, z; \xi, \eta, \zeta)) ds \\ = \begin{cases} n_j & \text{when } j = 1, 6 \\ -\frac{\partial \phi_0}{\partial n} & \text{when } j = 7 \end{cases} \quad \dots (30) \end{aligned}$$

This is similar to the infinite fluid problem formulated by Hess and Smith (8). In equation (30) one has to exclude the integration of the source part of the Green's function over the immediate neighbourhood of each point $(\xi, \eta, \zeta) = (x, y, z)$ on the surface S where the integral is evaluated. The contribution to the normal derivative from the immediate neighbourhood of (x, y, z) is taken care of by the term $-2\pi Q_j(x, y, z)$.

Equation (30) is solved by approximating the body surface by a large number of plane quadrilateral elements, over each of which the source density is assumed constant. This transforms the integral equation into a set of linear algebraic equations in the unknown values of the source density on the elements. The approach is the same as used by Hess and Smith (8), the only difference being that we have selected the centroid of each quadrilateral as the point where the Green's function and its derivative are evaluated, while Hess and Smith used the null point, i.e. the point where the velocity component in the plane of the surface element due to the source distribution of that element is zero. This difference is not significant and it is not necessarily a more correct refinement to use the null point instead of the centroid. The formulae for the integrated values of the derivatives of the sources over a quadrilateral have been derived by Hess and Smith. We adopted the criterion given by them to determine when the quadrilateral can be replaced by a source alone. Otherwise we used the integrated values. The same procedure was followed for the images of the source over the free surface and the sea bottom. For the other parts of the derivative of the Green's function we assumed constant values over each quadrilateral. The numerical work can be considerably reduced by taking into account symmetry properties. If the body has one plane of symmetry (which is the x - z plane) the source density has to be symmetric about this plane when $j = 1, 3$ and 5 . Further, when $j = 2, 4$ and 6 the source density is asymmetric about the same plane. When $j = 7$ we can split the source density into a symmetric and an asymmetric part. When the body has both the x - z -plane and the y - z -plane as planes of symmetry, then the source density will be symmetric about the x - z -plane and asymmetric about the y - z -plane for $j = 1$ and 5 . Further, when $j = 3$ the source density is symmetric, about both the x - z -plane and y - z -plane. When $j = 2$ and 4 the source density is symmetric about the y - z -plane and asymmetric about the x - z -plane. When $j = 6$ the source density is asymmetric about both the x - z -plane and the y - z -plane. Finally, for $j = 7$ we can split the source density into four parts in the same way as mentioned above. Thus, when there is only one plane of symmetry it is necessary to only satisfy the integral equation for positive x -values on the body surface S . When both the x - z -plane and y - z -plane are planes of symmetry it is only necessary to satisfy the integral equations for positive x - and y -values on S .

The integral equations (30) may not always yield a solution. For certain irregular frequencies (see John (9)) the method fails. This problem has been studied in the two-dimensional case by Faltinsen (10). However, as long as the body has no forward speed and there is no current, it is expected that the irregular frequencies will not present any problem. The irregular frequencies are furthermore expected to lie above the frequency range of interest. It should be noted that there exists no irregular frequencies for totally submerged bodies.

When the source densities Q_j have been found, the normalized potentials ϕ_j may be obtained from equation (22). The integration procedure is similar as explained in connection with the solution of the integral equation (30). We then need a method to integrate sources over a quadrilateral. This has been shown in Appendix 2.

We can now use Bernoulli's equation to obtain the pressure and, by definition, the added mass and damping coefficients A_{kj} and B_{kj} are as follows

$$A_{kj} = -\rho \operatorname{Re} \left\{ \iint_S \phi_j n_k ds \right\} \quad \dots (31)$$

$$B_{kj} = -\rho \omega \operatorname{Im} \left\{ \iint_S \phi_j n_k ds \right\} \quad \dots (32)$$

Here Re and Im mean the real and imaginary part, respectively. The indices k and j go from 1 to 6.

The wave exciting forces and moments F_i , $i = 1, 6$, are obtained from $\phi_0 e^{-i\omega t}$ and $\phi_7 e^{-i\omega t}$ by using the linearized Bernoulli's equation to obtain the pressure and integrating this pressure properly over the body surface S . We can now go back to the equations of motion (1)–(6) and solve for the motion. Having obtained the motion the velocity potential (11) is now determined. This enables us to find, for instance, the pressure at any point on the body. This may be used as the dynamic load in a quasi-static structural response calculation. Further, we can find the free-surface elevation at any point. The fluid velocity and acceleration can also be readily obtained. These may, for instance, be used in Morison equation-type calculations of forces and moments on small objects attached to the main body as appendages.

The motions, velocities, acceleration and pressure in irregular seas may now also be described. If we know the wave spectrum for the sea state we may use a linear superposition technique to obtain the response in an irregular sea (St. Denis and Pierson (11)).

4 DRIFT FORCES AND MOMENTS

So far we have studied the linear response in regular waves and neglected terms that are of higher than first order of magnitude in wave amplitude. However, in some cases the higher order terms are important, especially the second order horizontal drift force and moment. These terms may be used to calculate the mean drift force and moment on a body in an irregular sea (see for instance Gerritsma *et al.* (12)) and can also be used to calculate slowly varying excitation forces and moments on a body in an irregular sea (Hsu and Blenkarn (13)). Even if these forces are small they may cause large excursions of a free-floating body, since in such a case there are no restoring forces in the horizontal plane. Further, the frequency of the slowly-varying forces may very well lie in the resonance frequency range of an anchored body with the fatal consequence that the anchor

system fails. Thus, for dimensioning the anchor and dynamic positioning systems the study of drift forces and moments in regular waves is important.

Newman (14) has derived an exact expression for the horizontal drift force and moments in regular waves. He assumed infinite water depth, but his expressions can easily be generalized to finite water depth. Thus according to Newman

$$\bar{F}_x = -\int_{-\infty}^{\infty} \int [p \cos \theta + \rho V_r (V_r \cos \theta - V_\theta \sin \theta)] r d\theta dz \quad \dots (33)$$

$$\bar{F}_y = -\int_{-\infty}^{\infty} \int [p \sin \theta + \rho V_r (V_r \sin \theta + V_\theta \cos \theta)] r d\theta dz \quad \dots (34)$$

$$\bar{M}_z = -\rho \int_{-\infty}^{\infty} \int V_r V_\theta r^2 d\theta dz \quad \dots (35)$$

where the bars denote time average and the integration is over the surface S_∞ of a vertical circular cylinder of large radius r , that is extending from the free surface down to $z = -h$. \bar{F}_x and \bar{F}_y are the x - and y -components of the horizontal drift force and \bar{M}_z is the drift moment about the z -axis. We have used (r, θ, z) as cylindrical polar co-ordinates with $x = r \cos \theta$ and $y = r \sin \theta$. V_r and V_θ are the radial and tangential velocity components, respectively, and p is the dynamic pressure.

We will now approximate equations (33), (34) and (35) and only retain contributions that are of second order in the incident wave amplitude. To do this we only need to know the velocity potential to first order in wave amplitude. Using equations (11), (12), (22) and an asymptotic expansion of the Green's function expression (23), we may write

$$\begin{aligned} \phi \sim & \frac{g\zeta_a}{\omega} \frac{\cosh k(z+h)}{\cosh kh} e^{i(kx \cos \beta + ky \sin \beta - \omega t)} \\ & + F(\theta) e^{i\phi(\theta)} \cosh(k(z+h)) \sqrt{\left(\frac{1}{r}\right)} e^{i(kr - \omega t)} \quad \dots (36) \end{aligned}$$

Here $F(\theta)$ is real and $F(\theta) e^{i\phi(\theta)}$ is given by

$$\begin{aligned} F(\theta) e^{i\phi(\theta)} = & \frac{2\pi(v^2 - k^2)}{k^2 h - v^2 h + v} \sqrt{\left(\frac{2}{\pi k}\right)} e^{-i3\pi/4} \\ & \times \iint_S Q(\xi, \eta, \zeta) \cosh[k(\zeta+h)] e^{-ik\xi \cos \theta - ik\eta \sin \theta} ds \quad \dots (37) \end{aligned}$$

Further

$$Q(\xi, \eta, \zeta) = Q_7 + \sum_{i=1}^6 Q_i(-i\omega) \bar{\eta}_i \quad \dots (38)$$

Here $\bar{\eta}_i$ is defined by

$$\eta_i = \bar{\eta}_i e^{-i\omega t} \quad \dots (39)$$

where η_i , $i = 1, 6$ are the six modes of motion.

As shown in Appendix 3 we will get the following expressions for drift-force and moment

$$\begin{aligned} \left\{ \begin{array}{l} \bar{F}_x \\ \bar{F}_y \end{array} \right\} = & -\frac{\rho}{2} \frac{\omega\zeta_a}{\sinh kh} \sqrt{\left(\frac{2\pi}{k}\right)} \left(\frac{1}{4} \sinh 2kh + \frac{kh}{2} \right) \\ & \times 2\bar{F}(\beta) \cos \left(\phi(\beta) + \frac{\pi}{4} \right) \left\{ \begin{array}{l} \cos \beta \\ \sin \beta \end{array} \right\} \end{aligned}$$

$$-\frac{\rho}{2}k\left(\frac{1}{4}\sinh 2kh + \frac{kh}{2}\right)\int_0^{2\pi} F^2(\theta)\begin{Bmatrix} \cos\theta \\ \sin\theta \end{Bmatrix}d\theta \quad \dots(40)$$

$$\begin{aligned} \bar{M}_z &= \left[\frac{1}{k}\frac{\sinh 2kh}{4} + \frac{h}{2}\right]\cdot\left\{-\frac{\omega\zeta_a}{\sinh kh}\sqrt{\left(\frac{2\pi}{k}\right)}\right. \\ &\times F'(\beta)\sin\left(\phi(\beta) + \frac{\pi}{4}\right) - \frac{\omega\zeta_a}{\sinh kh}\sqrt{\left(\frac{2\pi}{k}\right)} \\ &\times \phi'(\beta)F(\beta)\cos\left(\phi(\beta) + \frac{\pi}{4}\right) - \frac{k}{2} \\ &\left.\times\int_0^{2\pi} F^2(\theta)\phi'(\theta)d\theta\right\} \quad \dots(41) \end{aligned}$$

Where $\phi'(\beta)$ means $d\phi/d\theta$ evaluated at $\theta = \beta$.

5 COMPUTATIONS

A computer programme NV459 based on the three-dimensional source technique has been developed at Det norske Veritas. For a fixed structure in regular waves the programme calculates the total linear hydrodynamic forces and moments, horizontal drift forces and moments, pressure distribution on the body and pressure, fluid velocity and acceleration for any point in the fluid. No assumption about geometrical symmetry is necessary. Floating objects do, however, usually have at least one plane of symmetry. For such an object the programme calculates the added-mass and damping coefficients and motions in six degrees of freedom. The object is geometrically described by using offset points on the wetted surface of the body. Following the procedure of Hess and Smith (8) one then creates plane surface elements approximating the wetted surface of the body.

For an object having two planes of symmetry and using 48 plane elements to describe the total wetted surface of the body, it takes in the order of one minute CPU time on UNIVAC 1108 to solve the hydrodynamic problem for one wavelength. To solve the problem for the same wavelength with a different direction of propagation only a little additional CPU time is required.

For an object having only one plane of symmetry and using a total of 48 plane elements, the computer time is 2 min CPU on UNIVAC 1108 for one wavelength. Similarly, for no plane of symmetry and a total of 48 plane elements the computer time is 4 min CPU. The computer time increases approximately as the square of the number of plane elements.

We have compared the computer programme with other analytical solutions, computer results and experiments and in general we have found very good agreement using a total of 48 plane elements. But in some cases, when calculating moments, we found it necessary to increase the number of plane elements.

The computer programme NV417 has also been used. This programme is based on the method of Salvesen, *et al.* (15) and calculates ship motions and wave loads for regular waves of any direction of propagation. For zero speed it reduces to a conventional strip theory. The two-dimensional velocity potentials are calculated using either the Lewis' form technique or the Frank Closefit Method.

In this report we show computations for two floating boxes. The boxes have length and beam equal to 90 m and the drafts were 20 m and 40 m full-scale. Further details are presented in Table 1. The water depth is infinite. The directions of wave propagations were $\beta = 0^\circ$ and 45° . The range of periods T chosen for the incoming waves was from 8–20 s. full-scale.

The strip theory programme NV417 was used for $\beta = 0^\circ$. The strips were placed in the lengthwise direction. A similar procedure has been used by Kim *et al.* (16) for the motions of a barge of length/beam ratio equal to 1.5 and with good results.

Table 1. Geometrical Data for Floating Box. $L = 90$ m, $B = 90$ m

	Draft = 40 m	Draft = 20 m
$C.G(x_G, y_G, z_G)$	0, 0, 10.62 m	0, 0, 8.82 m
k_x	33.04 m	37.32 m
k_y	32.09 m	33.30 m
k_z	32.92 m	40.08 m

The added mass and damping coefficients are presented in Figs 3–16.

The agreement between calculated values by the strip theory programme NV417 and the three-dimensional programme NV459 is generally not good and this was to be expected. The difference between the yaw-added masses of the two programmes is especially large.

The exciting forces and moments are presented in the form of amplitudes $|F_i|$ and phase angles α_i . They can be written in a time-dependent form as,

$$|F_i| \sin(\omega t + \alpha_i)$$

The incoming wave can be written as,

$$\zeta_a \sin(\omega t - kx \cos \beta - ky \sin \beta)$$

A positive phase angle, therefore, indicates that the force leads the wave height at the origin.

Exciting forces and moments for the box are presented in Figs 17–26.

The motions are presented in the form of amplitudes $|\eta_i|$ and phase angles α'_i . They can be written in a time-dependent form as,

$$|\eta_i| \sin(\omega t + \alpha'_i)$$

and we note that a positive phase angle indicates that the motion leads the wave height at the origin. Motions of the free-floating box are presented in Figs 30–37.

Drift forces are presented in Figs 27–29. The asymptotic values for small periods are also indicated. Expressions for these have been derived by Maruo (17). Assuming that the waves are propagating along the positive x -axis and that the body has vertical sides at the free surface, Maruo derived the following asymptotic expression for the drift force in the x -direction when $T \rightarrow 0$.

$$F_x = \frac{1}{2}\rho g \zeta_a^2 \int_{-b}^b \sin^2 \alpha dy$$

Here α is the slope of the tangent of the waterplane curve with respect to the x -axis. Further, $2b$ is the beam of the body and the integration is along the y -axis. In our case, for a heading angle $\beta = 0^\circ$, we get,

$$F_x = 0.5\rho g \zeta_a^2 \cdot L$$

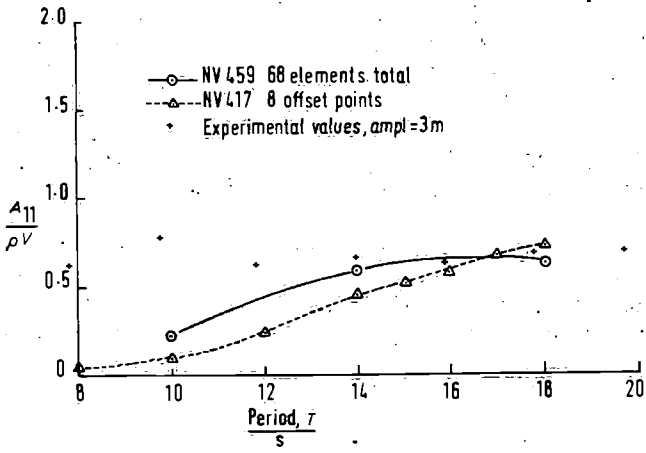


Fig. 3. Surge added-mass coefficients for floating box ($L \times B \times d = 90 \text{ m} \times 90 \text{ m} \times 20 \text{ m}$). Infinite water depth

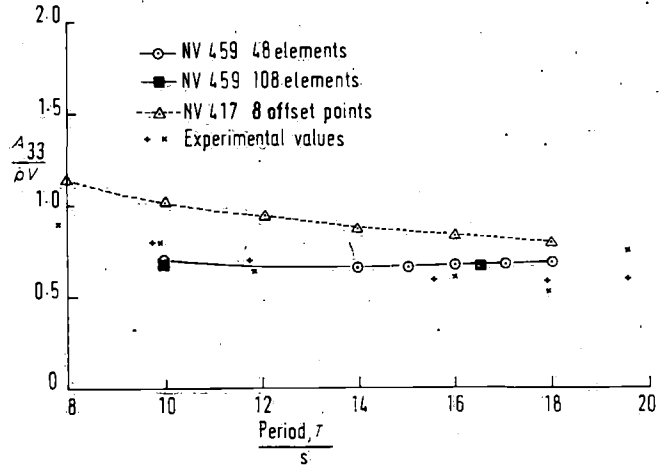


Fig. 6. Heave added-mass coefficients for floating box ($L \times B \times d = 90 \text{ m} \times 90 \text{ m} \times 40 \text{ m}$). Infinite water depth

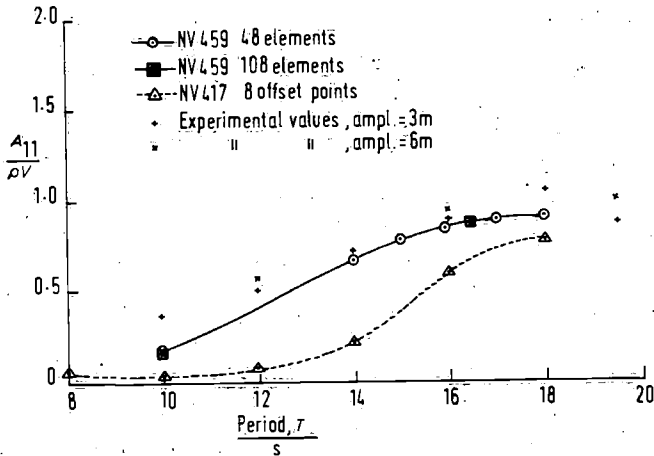


Fig. 4. Surge added-mass coefficients for floating box ($L \times B \times d = 90 \text{ m} \times 90 \text{ m} \times 40 \text{ m}$). Infinite water depth

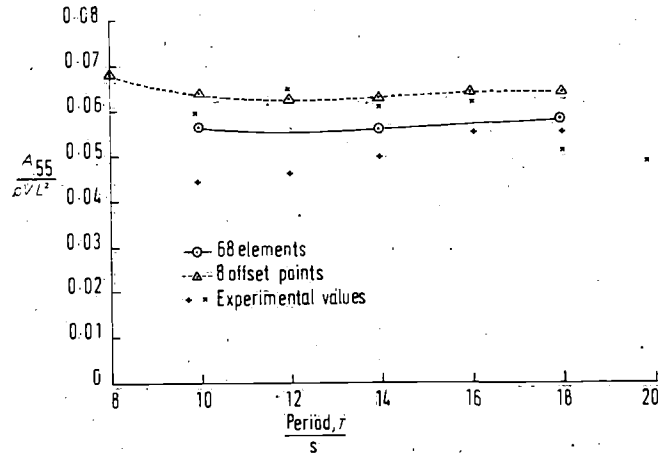


Fig. 7. Pitch added-mass coefficients for floating box ($L \times B \times d = 90 \text{ m} \times 90 \text{ m} \times 20 \text{ m}$). Infinite water depth

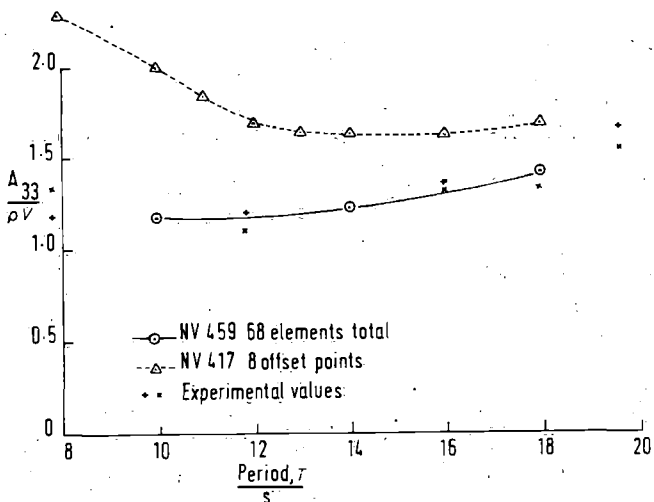


Fig. 5. Heave added-mass coefficients for floating box ($L \times B \times d = 90 \text{ m} \times 90 \text{ m} \times 20 \text{ m}$). Infinite water depth

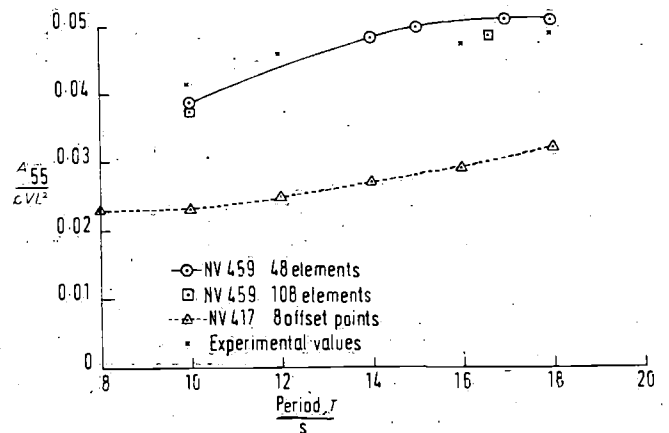


Fig. 8. Pitch added-mass coefficients for floating box ($L \times B \times d = 90 \text{ m} \times 90 \text{ m} \times 40 \text{ m}$). Infinite water depth

MOTIONS OF LARGE STRUCTURES IN WAVES AT ZERO FROUDE NUMBER

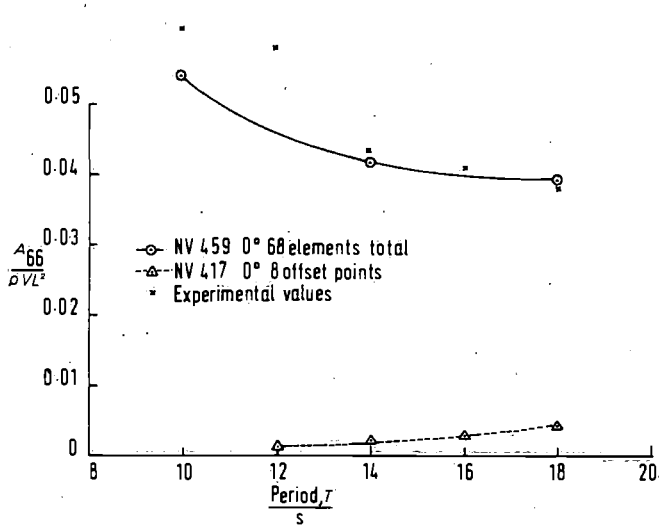


Fig. 9. Yaw added-mass coefficients for floating box ($L \times B \times d = 90 \text{ m} \times 90 \text{ m} \times 20 \text{ m}$). Infinite water depth

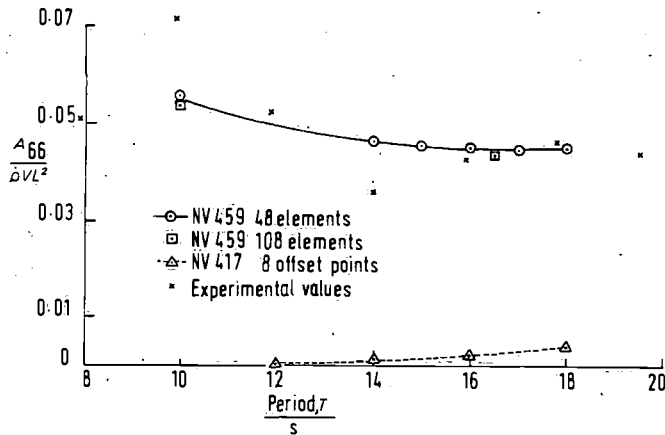


Fig. 10. Yaw added-mass coefficients for floating box ($L \times B \times d = 90 \text{ m} \times 90 \text{ m} \times 40 \text{ m}$). Infinite water depth

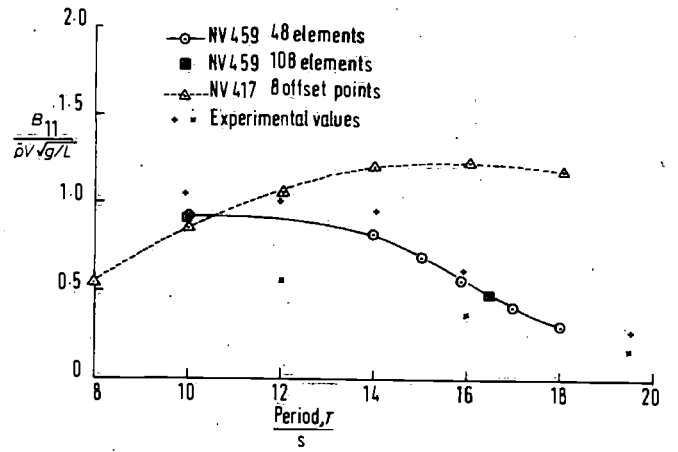


Fig. 12. Surge damping coefficients for floating box ($L \times B \times d = 90 \text{ m} \times 90 \text{ m} \times 40 \text{ m}$). Infinite water depth

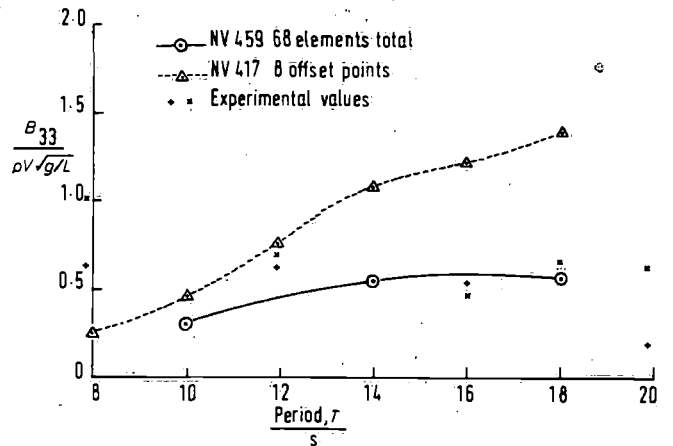


Fig. 13. Heave damping coefficients for floating box ($L \times B \times d = 90 \text{ m} \times 90 \text{ m} \times 20 \text{ m}$). Infinite water depth heave-heave damping coefficients

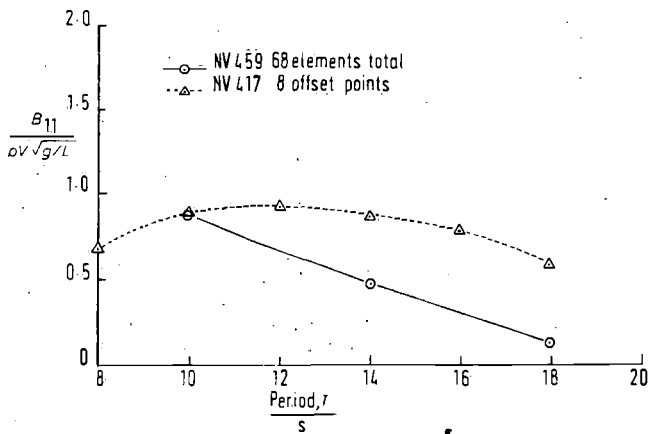


Fig. 11. Surge damping coefficients for floating box ($L \times B \times d = 90 \text{ m} \times 90 \text{ m} \times 20 \text{ m}$). Infinite water depth

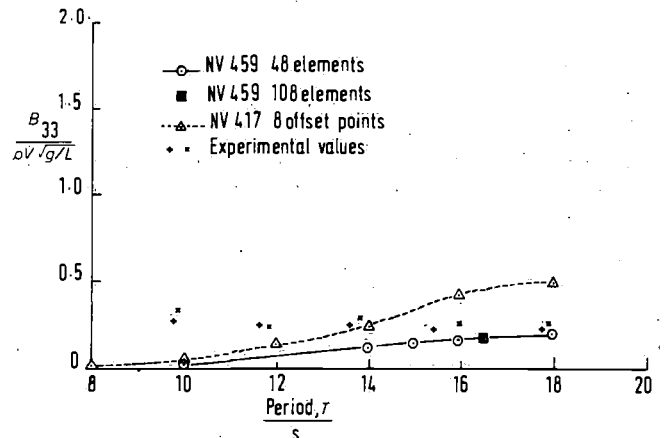


Fig. 14. Heave damping coefficients for floating box ($L \times B \times d = 90 \text{ m} \times 90 \text{ m} \times 40 \text{ m}$). Infinite water depth

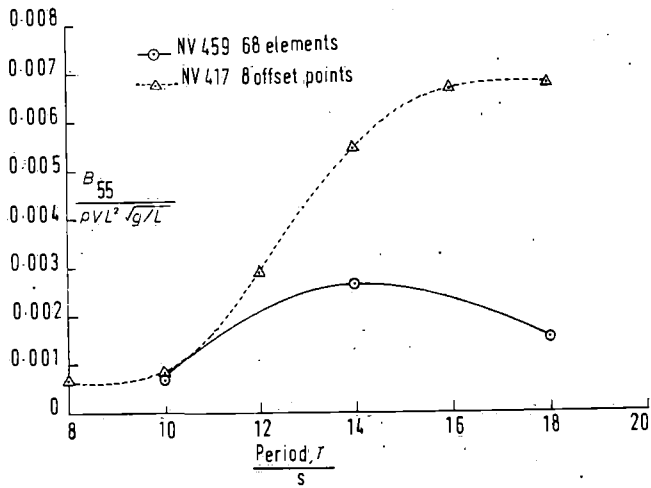


Fig. 15. Pitch damping coefficients for floating box ($L \times B \times d = 90 \text{ m} \times 90 \text{ m} \times 20 \text{ m}$). Infinite water depth

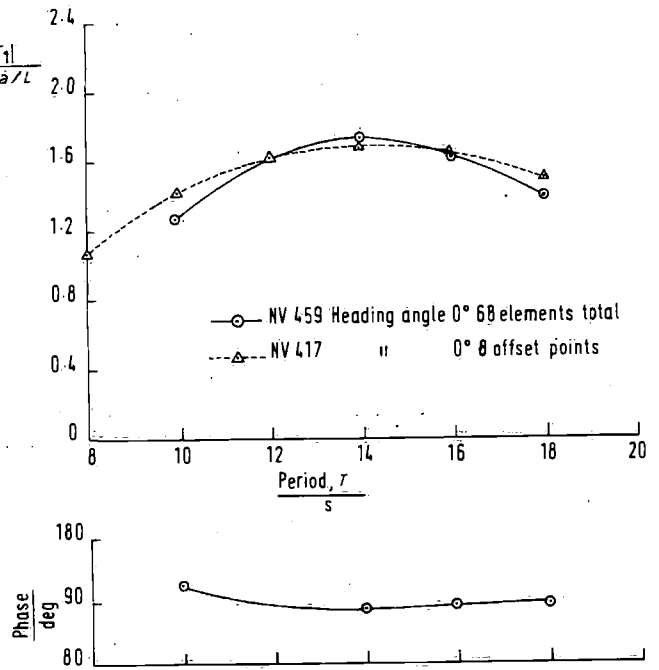


Fig. 17. Exciting force on floating box ($L \times B \times d = 90 \text{ m} \times 90 \text{ m} \times 20 \text{ m}$). Infinite water depth, amplitudes and phases

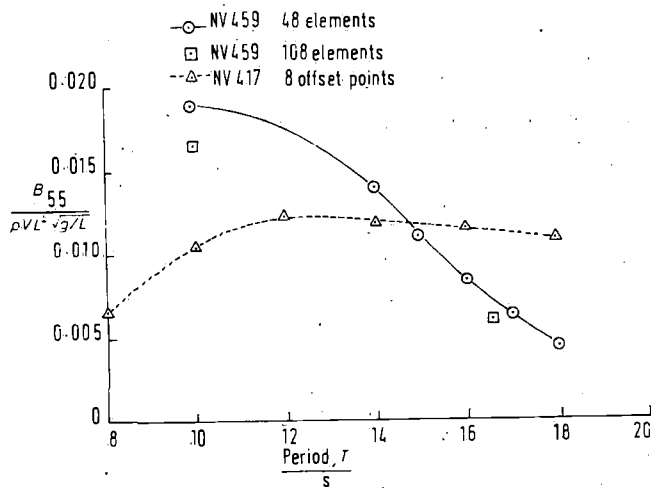


Fig. 16. Pitch damping coefficients for floating box ($L \times B \times d = 90 \text{ m} \times 90 \text{ m} \times 40 \text{ m}$). Infinite water depth

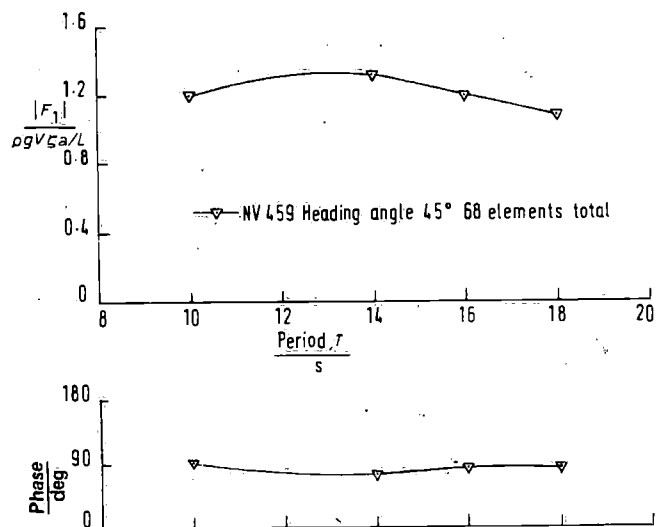


Fig. 18. Exciting force on floating box ($L \times B \times d = 90 \text{ m} \times 90 \text{ m} \times 20 \text{ m}$). Infinite water depth, amplitudes and phases

MOTIONS OF LARGE STRUCTURES IN WAVES AT ZERO FROUDE NUMBER

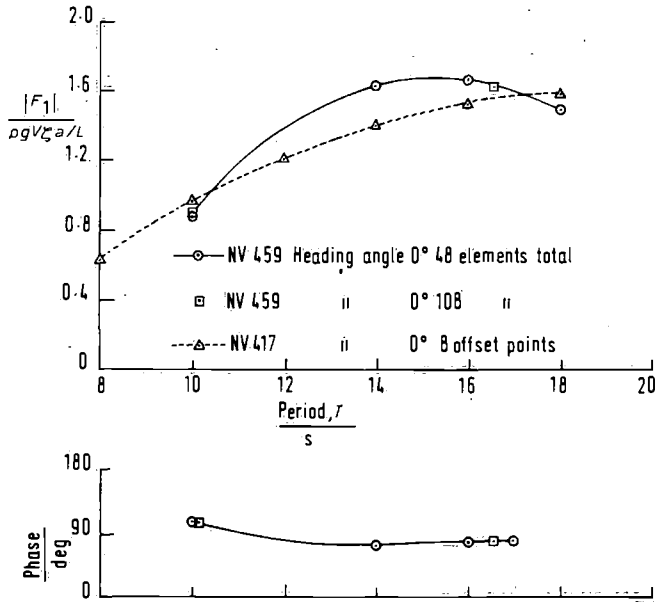


Fig. 19. Exciting force on floating box ($L \times B \times d = 90 \text{ m} \times 90 \text{ m} \times 40 \text{ m}$). Infinite water depth, amplitudes and phases

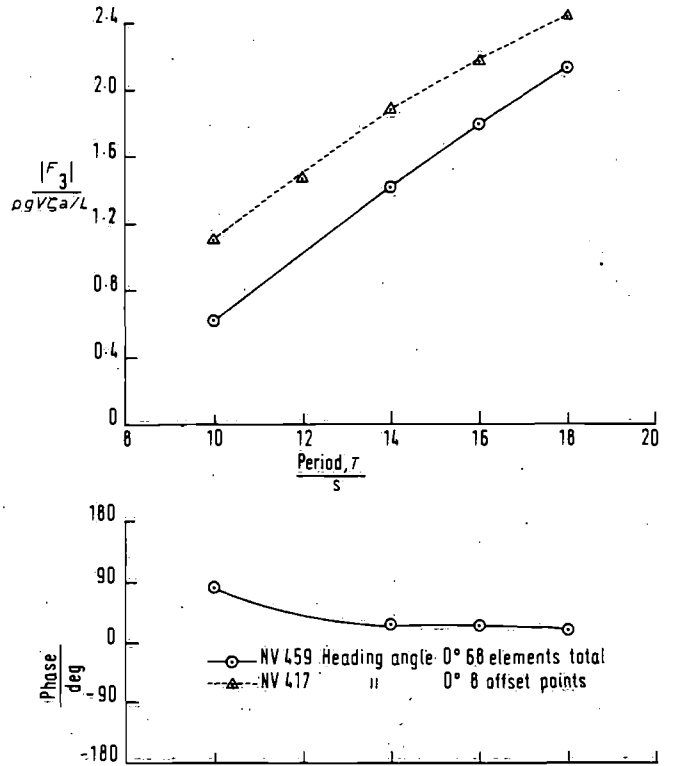


Fig. 21. Exciting force on floating box ($L \times B \times d = 90 \text{ m} \times 90 \text{ m} \times 20 \text{ m}$). Infinite water depth, amplitudes and phases

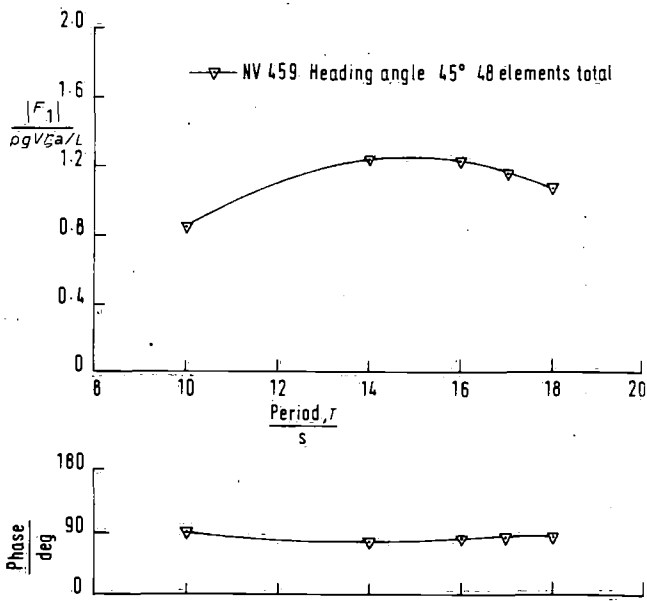


Fig. 20. Exciting force on floating box ($L \times B \times d = 90 \text{ m} \times 90 \text{ m} \times 40 \text{ m}$). Infinite water depth, amplitudes and phases

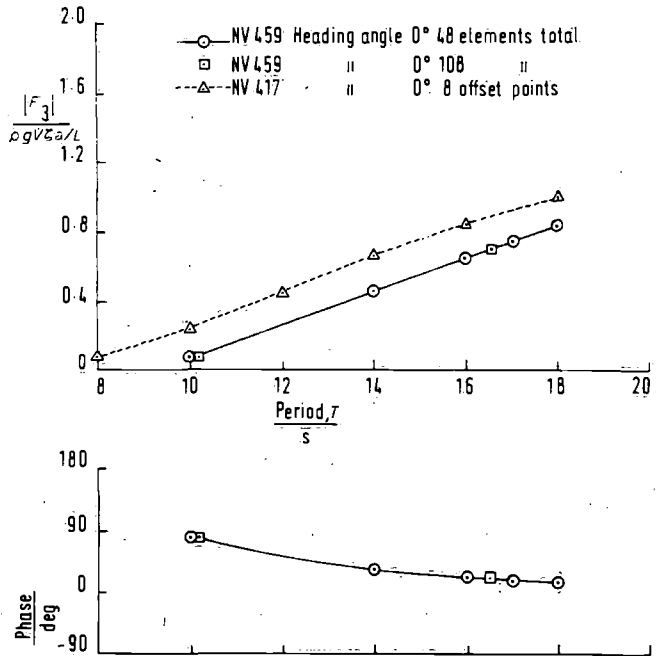


Fig. 22. Exciting force on floating box ($L \times B \times d = 90 \text{ m} \times 90 \text{ m} \times 40 \text{ m}$). Infinite water depth, amplitudes and phases

MARINE VEHICLES

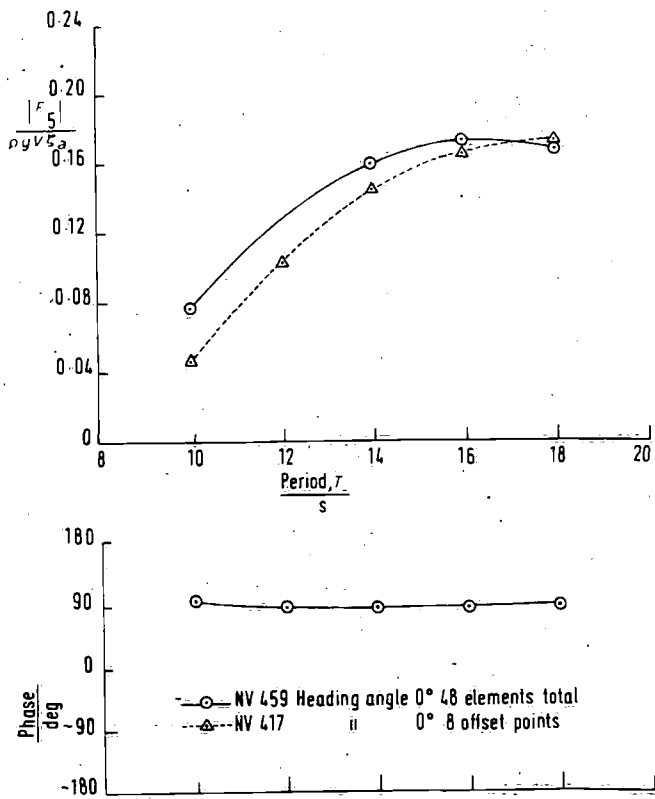


Fig. 23 Exciting moment on floating box ($L \times B \times d = 90 \text{ m} \times 90 \text{ m} \times 20 \text{ m}$). Infinite water depth, amplitudes and phases

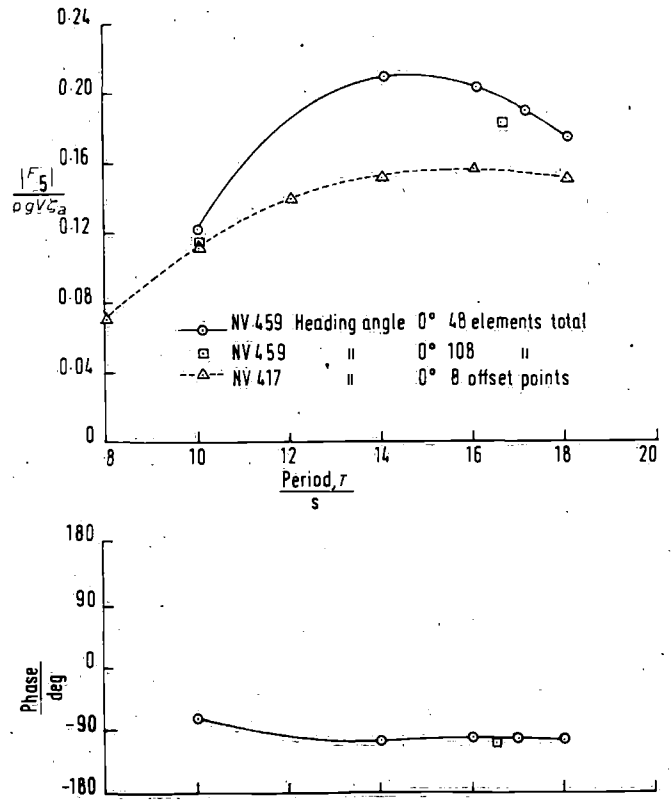


Fig. 25 Exciting moment on floating box ($L \times B \times d = 90 \text{ m} \times 90 \text{ m} \times 40 \text{ m}$). Infinite water depth, amplitudes and phases

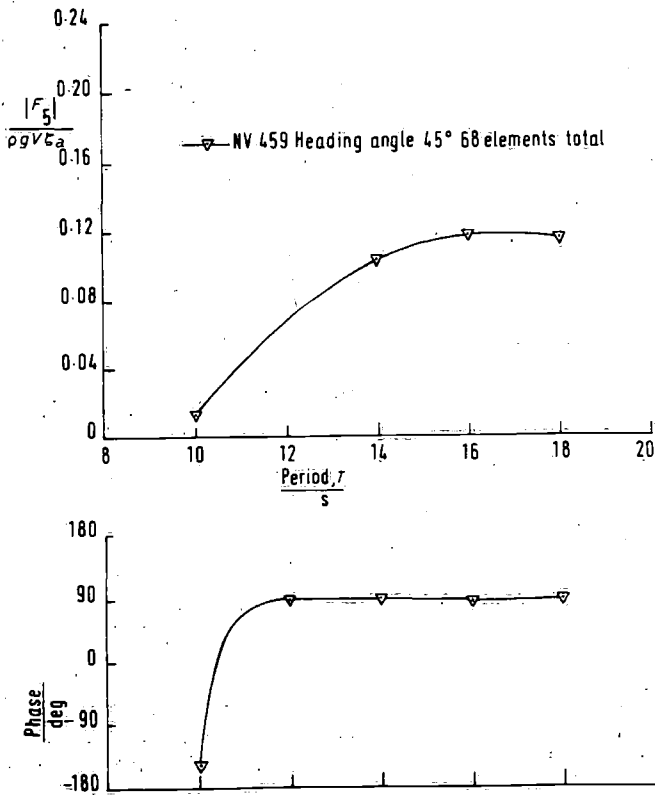


Fig. 24 Exciting moment on floating box ($L \times B \times d = 90 \text{ m} \times 90 \text{ m} \times 20 \text{ m}$). Infinite water depth, amplitudes and phases

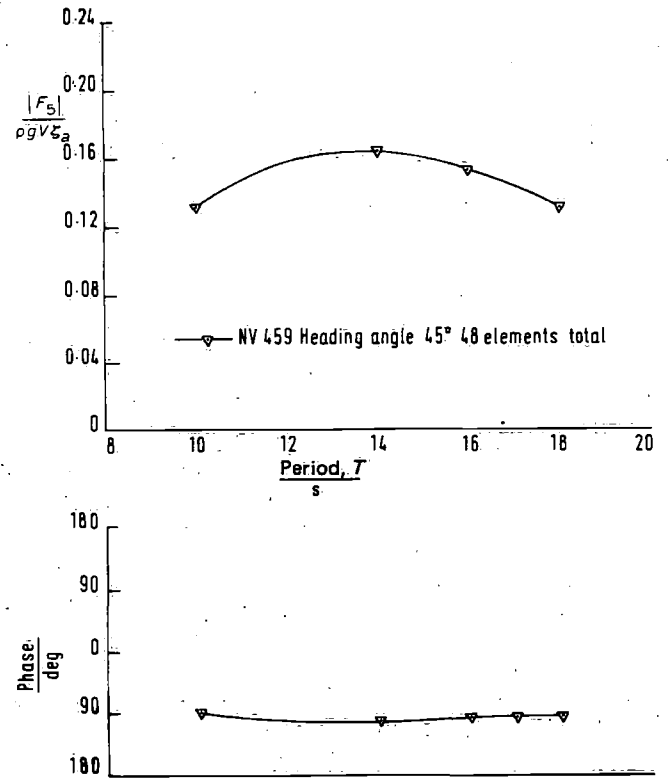


Fig. 26 Exciting moment on floating box ($L \times B \times d = 90 \text{ m} \times 90 \text{ m} \times 40 \text{ m}$). Infinite water depth, amplitudes and phases

MARINE VEHICLES

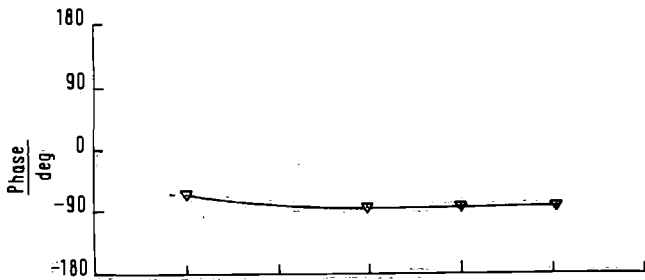
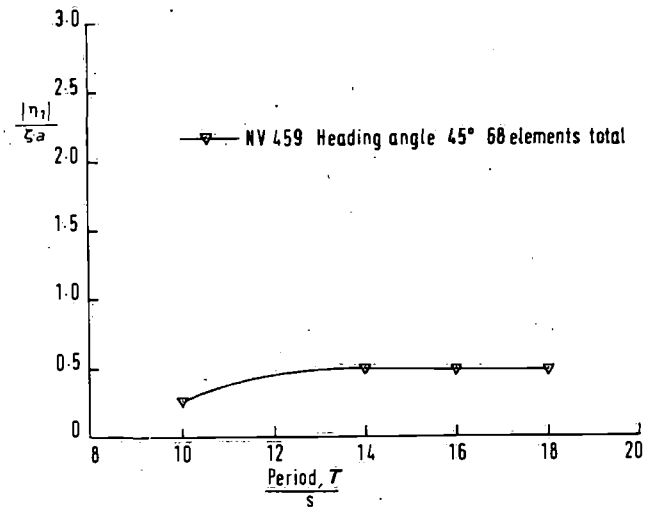


Fig. 31. Motions of floating box ($L \times B \times d = 90 \text{ m} \times 90 \text{ m} \times 20 \text{ m}$). Infinite water depth, amplitudes and phases

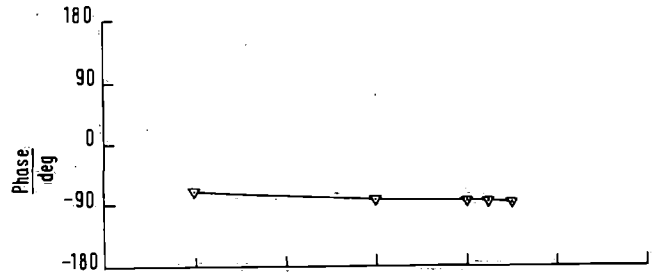
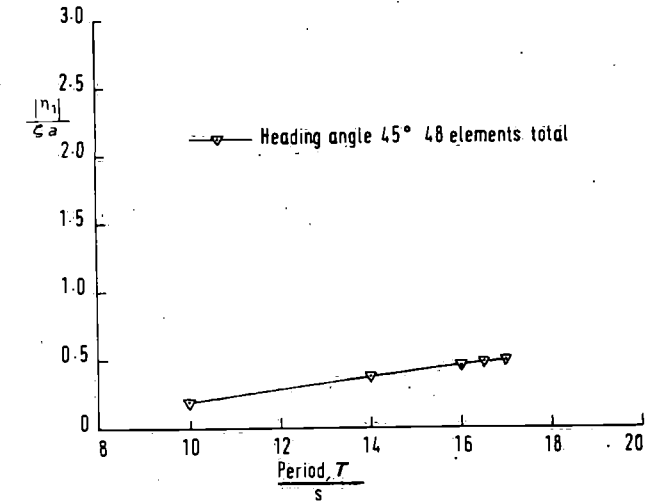


Fig. 33. Motions of floating box ($L \times B \times d = 90 \text{ m} \times 90 \text{ m} \times 40 \text{ m}$). Infinite water depth, amplitudes and phases

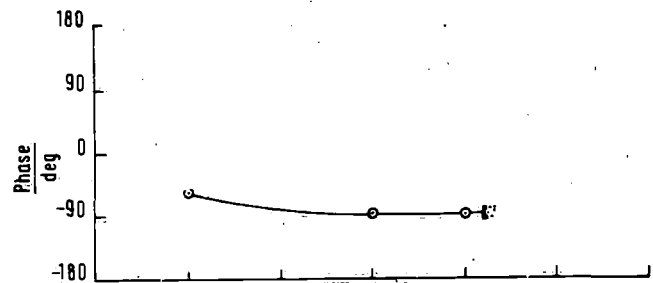
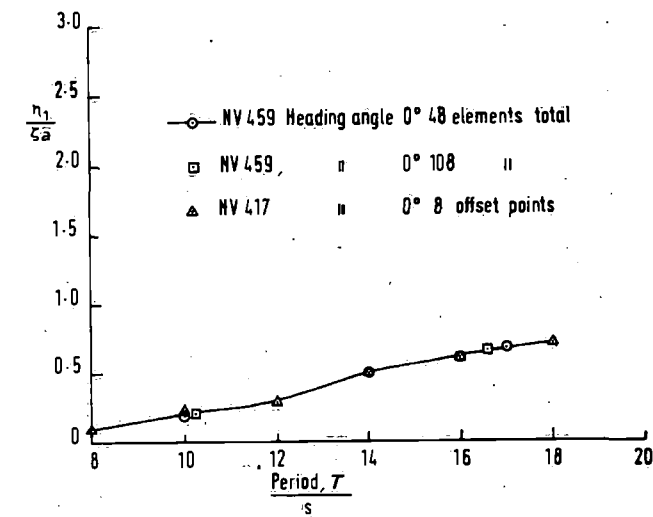


Fig. 32. Motions of floating box ($L \times B \times d = 90 \text{ m} \times 90 \text{ m} \times 40 \text{ m}$). Infinite water depth, amplitudes and phases

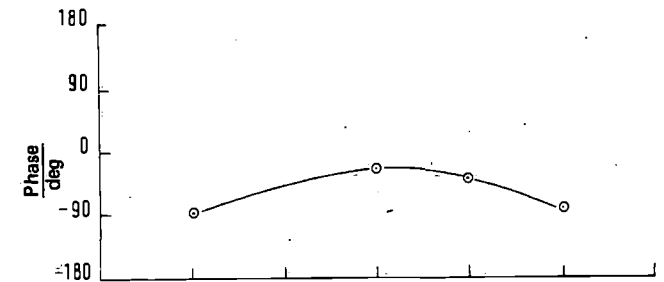
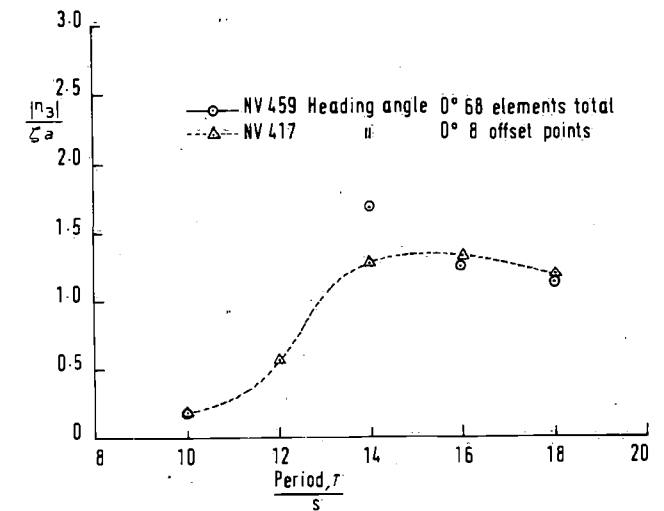


Fig. 34. Motions of floating box ($L \times B \times d = 90 \text{ m} \times 90 \text{ m} \times 20 \text{ m}$). Infinite water depth, amplitudes and phases

MOTIONS OF LARGE STRUCTURES IN WAVES AT ZERO FROUDE NUMBER

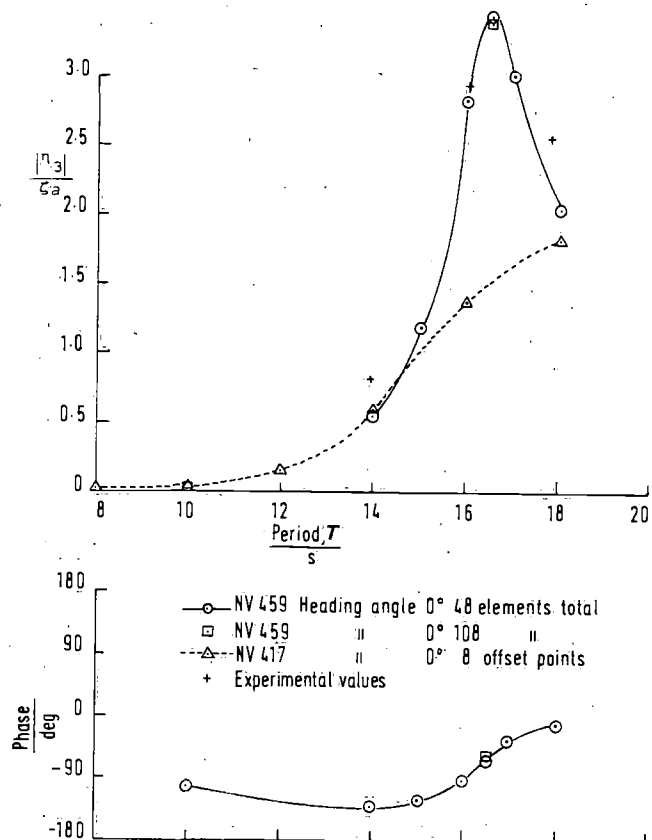


Fig. 35. Motions of floating box ($L \times B \times d = 90 \text{ m} \times 90 \text{ m} \times 40 \text{ m}$). Infinite water depth, amplitudes and phases

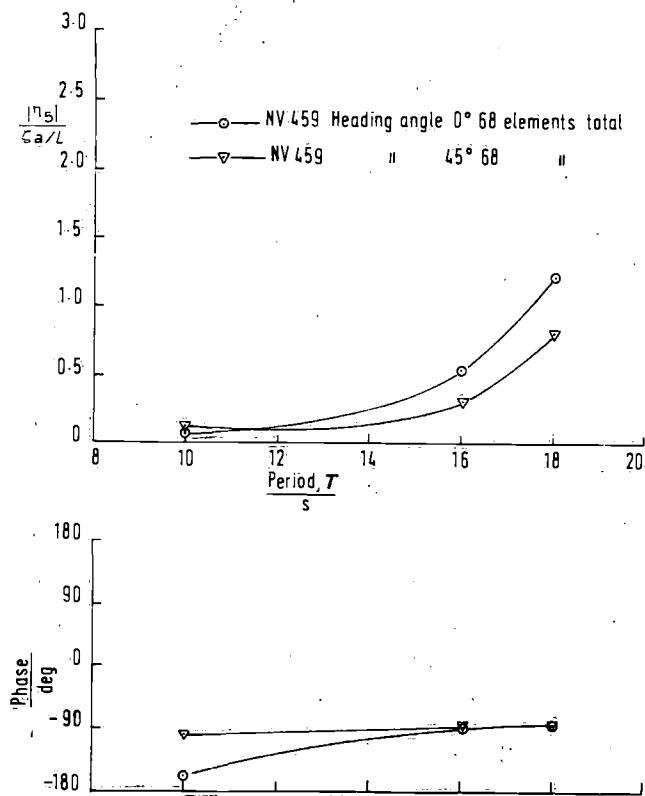


Fig. 36. Motions of floating box ($L \times B \times d = 90 \text{ m} \times 90 \text{ m} \times 20 \text{ m}$). Infinite water depth, amplitudes and phases

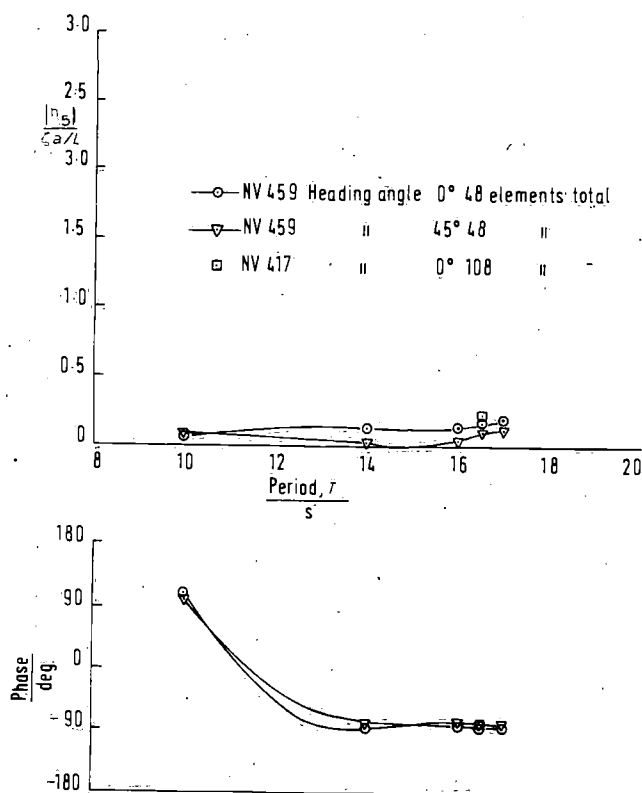


Fig. 37. Motions of floating box ($L \times B \times d = 90 \text{ m} \times 90 \text{ m} \times 40 \text{ m}$). Infinite water depth, amplitudes and phases

For both boxes this asymptotic value agrees quite well with our calculations.

Introducing an x' -axis along the direction of wave propagation we may use Maruo's formula also for heading angle $\beta = 45^\circ$. We then get,

$$F_x = \frac{\sqrt{2}}{8} \rho g \zeta_a^2 \cdot L$$

for the drift force along our permanent x -axis. Again the asymptotic value agrees very well with our computations.

We may further note that the effect of the motion on the drift forces is small for the lower periods. For the floating box of draft 40 m and close to the heave resonance frequency, there is a strong dependence on the motions. This may be expected since the maximum immersion of the body is increased due to large relative vertical motion between wave and body. For the floating box of draft 20 m there is a strong dependence on the motions for the larger periods. The body moves more or less as a water particle for these periods and the drift force is therefore very small.

6 CONCLUSIONS

A theoretical method has been presented that describes the motions, in all six degrees of freedom, of large floating structures in waves when the Froude number is zero. The method also gives the hydrodynamic pressures and the horizontal drift forces.

The method of analysis used is based on a three-dimensional source technique with the sources distributed

on the surface of the body. The drift forces are derived from momentum equations.

Numerical calculations and experimental results for the case of a floating box of dimensions 90 m × 90 m and a draught of 20 m and 40 m show very good agreement in the measured quantities. On the basis of this comparison one may conclude that the method does indeed provide a solution to the dynamic analysis of large three-dimensional structures in waves, subject, of course, to the usual limitations of the linearized theory.

It may seem attractive to try to apply a two-dimensional strip theory to the analysis of the structures of concern here. This has been done for the box mentioned above and the results show that this method of approach cannot be used in the dynamic analysis of such structures. Only a three-dimensional method of analysis, as given in this paper, will be adequate.

Experiment

For the purpose of verifying computed values of added mass and damping coefficients of the 90 m × 90 m box at draughts of 20 m and 40 m a series of tests were performed in the model basin of the University of Trondheim with a model built to scale 1:100. The model was oscillated in heave, surge, pitch and yaw at amplitudes of 3 cm and 0.05 rad respectively. Some tests were also made at twice these amplitudes to check on linearity.

The experimental results agree generally very well with the theoretical predictions. Where deviations from theoretical values are most pronounced it was found that these were probably caused by the fact that it was not always possible to provide a pure one degree of freedom motion to the model. This was true in particular for the cases of surge and yaw in the range of low periods.

In regard to damping, deviations from theoretical values may seem to be significant in this range of periods. This may be due to viscous effects, but it should be pointed out that damping is small and difficult to determine experimentally with any great degree of accuracy. Only a few degrees of error in the measurement of the phase angle will, for instance, result in large variations in the damping force. For the same reason it was found that damping in yaw and pitch were much higher than theoretical predictions indicated, and no experimental values are therefore given.

A model to scale 1:60 was also built for the purpose of determining excitation forces. These experiments were not successful due to instrumentation failures, and the tests will therefore have to be repeated. A free-floating test did, however, provide us with experimental data on heave motions and drift forces. Again one can conclude that correlation between theory and experiments is good.

7 ACKNOWLEDGMENT

The authors are particularly indebted to Mr A. Løken of Det Norske Veritas for his contribution in programming and numerical computations. Also the assistance of the staff at the Ship Model Basin in Trondheim is fully acknowledged, as is the work of Mr T. Mikkelsen and Mr J. Knudsen, students at the University in Trondheim, in analyzing experimental data.

APPENDIX 1

Numerical evaluation of the Green's function Equation (24) can be rewritten as

$$G(x, y, z; \xi, \eta, \zeta) = \frac{1}{R} + \frac{1}{R^1} + \frac{1}{\sqrt{[(x - \xi)^2 + (y - \eta)^2 + (z + \zeta)^2]}} + PV \int_0^{u_1} \frac{2(ku + v) e^{-khu} \cosh [k(\zeta + h)u]}{u \sinh(khu) - (v/k) \cosh(khu)} J_0(kr_1 u) du - \int_0^{u_1} e^{(z+\zeta)ku} J_0(kur_1) k du + \int_{u_1}^{\infty} \frac{2v e^{ku(z+\zeta)} J_0(kr_1 u) du}{u - v/k} + i \frac{2\pi(k^2 - v^2) \cosh [k(\zeta + h)] \cosh [k(z + h)]}{k^2 h - v^2 h + v} J_0(kr_1) \quad \dots(42)$$

We have here disjoined the image source with respect to the free surface by making use of the fact that $((x - \xi)^2 + (y - \eta)^2 + (z + \zeta)^2)^{-\frac{1}{2}}$

$$= \int_0^{\infty} e^{(z+\zeta)\mu} J_0(\mu r_1) d\mu \quad \dots(43)$$

(see Gradshteyn and Ryzhik (18)). The limit of integration u_1 in equation (42) must satisfy the following conditions:

$$(i) \quad u_1 \geq 2,$$

due to numerical methods used in the evaluation of the principal value integral,

$$(ii) \quad u_1 \geq 4.5/kh$$

so that we may with sufficient accuracy set

$$\left. \begin{array}{l} \cosh khu \\ \sinh khu \end{array} \right\} \sim \frac{1}{2} e^{khu} \text{ for } u \geq u_1$$

The principal value integration in equation (42) has been calculated using the 'midpoint rule' and the procedure proposed by Monacella (19). The infinite integral in equation (42) can be converted into a finite integral by using the integral representation

$$J_0(kr_1 u) = \frac{1}{\pi} \int_0^{\pi} e^{ikr_1 u \cos \theta} d\theta \quad \dots(44)$$

(see Abramowitz and Stegun (20)). We may then write

$$\int_{u_1}^{\infty} \frac{2v e^{ku(z+\zeta)} J_0(kr_1 u) du}{u - v/k} = \frac{2v}{\pi} \int_0^{\pi} d\theta e^{v(z+\zeta) + ivr_1 \cos \theta} E_1 \left[- (k(z + \zeta) + ikr_1 \cos \theta) \left(u_1 - \frac{v}{k} \right) \right] \quad \dots(45)$$

where E_1 is the exponential integral as defined in Abramowitz and Stegun (20). The integral in equation (45) has been evaluated using the 'mid-point rule'.

APPENDIX 2

Integration of sources with constant density over a quadrilateral

We consider a plane quadrilateral source element lying in the x - y -plane as shown in Fig. 2.

The x - y or ξ - η co-ordinates of the four corner points defining the quadrilateral are (ξ_1, η_1) , (ξ_2, η_2) , (ξ_3, η_3) and (ξ_4, η_4) . It is desired to determine the velocity potential induced by this source element at a general point P in space having co-ordinates x, y, z . The value of the source density is set constant over the quadrilateral. The potential then becomes proportional to

$$\phi = \int_A \int \frac{1}{R} dA = \int_A \int \frac{d\xi d\eta}{\sqrt{[(x - \xi)^2 + (y - \eta)^2 + z^2]}} \quad \dots(46)$$

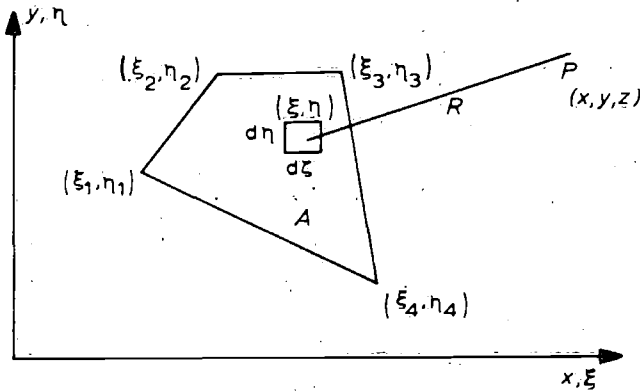


Fig. 2 Plane quadrilateral source element

Following a procedure similar to the one used by Hess and Smith (8) for the velocity components we obtain

$$\begin{aligned} \phi = & - \int_{\xi_1}^{\xi_2} d\xi \log(y - \eta_{12} \\ & + \sqrt{[(y - \eta_{12})^2 + (x - \xi)^2 + z^2]}) \\ & - \int_{\xi_2}^{\xi_3} d\xi \log(y - \eta_{23} \\ & + \sqrt{[(y - \eta_{23})^2 + (x - \xi)^2 + z^2]}) \\ & - \int_{\xi_3}^{\xi_4} d\xi \log(y - \eta_{34} \\ & + \sqrt{[(y - \eta_{34})^2 + (x - \xi)^2 + z^2]}) \\ & - \int_{\xi_4}^{\xi_1} d\xi \log(y - \eta_{41} \\ & + \sqrt{[(y - \eta_{41})^2 + (x - \xi)^2 + z^2]}) \quad \dots(47) \end{aligned}$$

Here

$$\eta_{ij} = \eta_i + \frac{\eta_j - \eta_i}{\xi_j - \xi_i} (\xi - \xi_i) \quad \dots(48)$$

We note that the integrand of the first integral is singular when $z = 0$, $\xi = x$ and $y - \eta_{12} < 0$. In this case we change the integral to read

$$\int_{\xi_1}^{\xi_2} d\xi \log((x - \xi)^2 + z^2) - \int_{\xi_1}^{\xi_2} d\xi \log[-(y - \eta_{12}) + \sqrt{(y - \eta_{12})^2 + (x - \xi)^2 + z^2}] \quad \dots(49)$$

The first integral of equation (49) can easily be integrated analytically (see Gradshteyn and Ryzhik (18)). The second integrand of equation (49) has no singularity in the integrand and no difficulties in the numerical integration are encountered. Difficulties with singularities in the integrand of the other integrals of equation (47) are handled in a similar manner.

APPENDIX 3

Derivation of second order drift force and moment

We shall show here how one can pass from equation (33), (34), (35) to equations (40) and (41), which are correct to second order in wave amplitude.

Using Bernoulli's equation we may write

$$\int_{-h}^{\zeta} p dz = \frac{\rho g}{2} \zeta^2 - \frac{\rho}{2} \int_{-h}^{\zeta} |V|^2 dz \quad \dots(50)$$

Here ζ is the free-surface elevation and V the fluid velocity vector which has the components (V_r, V_θ, V_z) in the cylindrical co-ordinate system. It is possible to show that

$$\begin{aligned} \frac{\rho g}{2} \zeta^2 = & \frac{\rho g}{2} \left\{ \frac{\zeta_a^2}{2} + \zeta_a F(\theta) \frac{\omega}{g} \cosh(kh) r^{-\frac{1}{2}} \right. \\ & \times \cos(kr(1 - \cos \theta \cos \beta - \sin \theta \sin \beta) + \phi(\theta)) \\ & \left. + \frac{1}{2} \frac{\omega^2}{g^2} F^2(\theta) \cosh^2 kh r^{-1} \right\} \quad \dots(51) \end{aligned}$$

$$\begin{aligned} \frac{\rho}{2} \int_{-h}^{\zeta} V_r^2 dz = & \frac{\rho}{2} \left[\frac{1}{k} \frac{\sinh 2kh}{4} + \frac{h}{2} \right] \\ & \times \left\{ \frac{1}{2} \frac{\omega^2 \zeta_a^2 \cos^2(\beta - \theta)}{\sinh^2 kh} + \frac{1}{8} F^2(\theta) r^{-3} + \frac{1}{2} F^2(\theta) k^2 r^{-1} \right. \\ & + \frac{1}{2} \omega \zeta_a \frac{\cos(\beta - \theta)}{\sinh kh} F(\theta) r^{-\frac{3}{2}} \\ & \times \sin(kr(\cos(\beta - \theta) - 1) - \phi(\theta)) \\ & \left. + \omega \zeta_a \frac{\cos(\beta - \theta)}{\sinh kh} F(\theta) kr^{-\frac{1}{2}} \right. \\ & \left. \times \cos[kr(\cos(\beta - \theta) - 1) - \phi(\theta)] \right\} \quad \dots(52) \end{aligned}$$

$$\begin{aligned} \frac{\rho}{2} \int_{-h}^{\zeta} V_\theta^2 dz = & \frac{\rho}{2} \left[\frac{1}{k} \frac{\sinh 2kh}{4} + \frac{h}{2} \right] \left\{ \frac{1}{2} \frac{\omega^2 \zeta_a^2 \sin^2(\theta - \beta)}{\sinh^2 kh} \right. \\ & + \frac{1}{2} r^{-3} (F'(\theta))^2 + \frac{1}{2} r^{-3} (F(\theta) \phi'(\theta))^2 + \frac{\omega \zeta_a}{\sinh kh} \\ & \times \sin(\theta - \beta) r^{-\frac{1}{2}} F'(\theta) \sin[kr(\cos(\theta - \beta) - 1) - \phi(\theta)] \\ & - \frac{\omega \zeta_a}{\sinh kh} \sin(\theta - \beta) r^{-\frac{1}{2}} F(\theta) \phi'(\theta) \\ & \left. \times \cos[kr(\cos(\theta - \beta) - 1) - \phi(\theta)] \right\} \quad \dots(53) \end{aligned}$$

$$\begin{aligned} \frac{\rho}{2} \int_{-h}^{\zeta} V_z^2 dz = & \frac{\rho}{2} \left[\frac{1}{k} \frac{\sinh 2kh}{4} - \frac{h}{2} \right] \left\{ \frac{1}{2} \frac{\omega \zeta_a^2}{\sinh^2 kh} \right. \\ & + \frac{1}{2} r^{-1} F^2(\theta) k^2 + \frac{\omega \zeta_a}{\sinh kh} r^{-\frac{1}{2}} F(\theta) k \\ & \left. \times \cos[kr(\cos(\theta - \beta) - 1) - \phi(\theta)] \right\} \quad \dots(54) \end{aligned}$$

$$\begin{aligned} \rho \int_{-h}^{\zeta} V_r V_\theta dz = & \rho \left[\frac{1}{k} \frac{\sinh 2kh}{4} + \frac{h}{2} \right] \left\{ \frac{1}{2} \frac{\omega^2 \zeta_a^2}{\sinh^2 kh} \right. \\ & \times \cos(\theta - \beta) \sin(\theta - \beta) - \frac{1}{2} \frac{\omega \zeta_a}{\sinh kh} \cos(\theta - \beta) \\ & \left. \times r^{-\frac{1}{2}} F'(\theta) \sin[kr(\cos(\theta - \beta) - 1) - \phi(\theta)] \right\} \end{aligned}$$

$$\begin{aligned}
& + \frac{1}{2} \frac{\omega \zeta_a}{\sinh kh} \cos(\theta - \beta) r^{-\frac{1}{2}} F(\theta) \phi'(\theta) \\
& \times \cos [kr(\cos(\theta - \beta) - 1) - \phi(\theta)] \\
& - \frac{1}{4} \frac{\omega \zeta_a}{\sinh kh} r^{-\frac{1}{2}} \bar{F}(\theta) \sin(\theta - \beta) \\
& \times \sin [(kr(\theta - \beta) - 1) - \phi(\theta)] - \frac{1}{4} r^{-\frac{3}{2}} F(\theta) F'(\theta) \\
& + \frac{1}{2} kr^{-2} F^2(\theta) \phi'(\theta) - \frac{1}{2} \frac{\omega \zeta_a}{\sinh kh} r^{-\frac{1}{2}} F(\theta) k \sin(\theta - \beta) \\
& \times \cos [kr(\cos(\theta - \beta) - 1) - \phi(\theta)] \} \dots (55)
\end{aligned}$$

Here $\bar{F}(\theta)$ and $\phi'(\theta)$ mean $dF/d\theta$ and $d\phi/d\theta$, respectively. Now by applying the method of stationary phase (Erdélyi (21)) we may write for large r

$$\begin{aligned}
& \int_0^{2\pi} g(\theta) \cos [kr(\cos(\theta - \beta) - 1) - \phi(\theta)] d\theta \\
& \sim \left(\frac{2\pi}{rk}\right)^{\frac{1}{2}} \left\{ g(\beta) \cos\left(\phi(\beta) + \frac{\pi}{4}\right) \right. \\
& \left. + g(\beta + \pi) \cos\left(-\phi(\beta + \pi) + \frac{\pi}{4} - 2kr\right) \right\} \dots (56)
\end{aligned}$$

where $g(\theta)$ is some arbitrary function. By using equations (50)–(56) we may write the drift forces and moments in the form of equations (40) and (41).

APPENDIX 4

REFERENCES

- (1) MORISON, J. R., O'BRIEN, M. P., JOHNSON, J. W. and SHAAF, S. A. 'The forces exerted by surface waves on piles', *Trans. Am. Petrol. Inst.* 1950 **189** (No. 2346).
- (2) LEBRETON, J. C. and CORMAULT, P. 'Wave action on slightly immersed structures, some theoretical and experimental considerations', *Proc. Symp. Research on Wave Action* 1969 4.
- (3) GARRISON, C. J. and SEETHARAMA RAO, V. Interactions of waves with submerged objects', *J. Waterways, Harbours Coastal Engng Div., ASCE* 1971 **97** (No. WW2) 259–277.
- (4) MILGRAM, J. H. and HALKYARD, J. E. 'Wave forces on large objects in the sea', *J. Ship Res.*, 1961.
- (5) VAN OORTMERSEN, G. 'Some aspects of very large offshore structures', *Proc. ONR Ninth Symposium on Naval Hydrodynamics* 1972.
- (6) LAMB, H. *Hydrodynamics*, 6th ed. 1932 (Cambridge University Press).
- (7) WEHAUSEN, J. V. and LAITONE, E. V. 'Surface waves', *Handbuch der Physik*, 9. 1969 (Springer-Verlag, Berlin).
- (8) HESS, J. L. and SMITH, A. M. O. 'Calculation of non-lifting potential flow about arbitrary three-dimensional bodies', Rep. No. E.S. 40622, 1962 (Douglas Aircraft Division, Long Beach, California). Also in abbreviated form in *J. Ship Res.*, 1964, 8.
- (9) JOHN, F. 'On the motion of floating bodies II', *Commun. pure appl. Math.* 1950, 3.
- (10) FALTINSEN, O. 'A study of the two-dimensional added-mass and damping coefficients by the Frank Close-Fit method', Det norske Veritas, Oslo, Norway, Rep. No. 69-10-S, 1969.
- (11) ST. DENIS, M. and PIERSON, W. J. 'On the motion of ships in confused seas', *Trans. SNAME*, 1953, 61.
- (12) GERRITSMAN, J., BOSCH, V. D. J. J. and BEUKELMAN, N. 'Propulsion in regular and irregular waves', *Int. Shipbuilding Progress* 1961.
- (13) HSU, F. H. and BLENKARN, K. A. 'Analysis of peak mooring force caused by slow vessel drift oscillation in random seas', *O.T.C.* 1970, Paper No. 1159.
- (14) NEWMAN, J. N. 'The drift force and moment on ships in waves', *J. Ship Res.* 1967.
- (15) SALVESEN, N., TUCK, E. O. and FALTINSEN, O. M. 'The ship motions and sea loads', *Trans. SNAME* 1970, 78.
- (16) KIM, CH. and CHOU, F. 'Hydrodynamic characteristics of barges', *Offshore Technology Conference, Houston* 1971.
- (17) MARUO, H. 'The drift of a body floating in waves', *J. Ship Res.* 1960.
- (18) GRADSHTEYN, I. S. and RYZHIK, I. M. *Tables of integrals, series and products* 1965 (Academic Press, New York and London).
- (19) MONACELLA, V. J. 'The disturbance due to a slender ship oscillating in waves in a fluid of finite depth', *J. Ship Res.* 1966 **10** (No. 4), 242–252.
- (20) ABRAMOWITZ, M. and STEGUN, I. A. *Handbook of mathematical functions* 1964 (National Bureau of Standards Mathematics Series, 55, Washington, D.C.).
- (21) ERDÉLYI, A. *Asymptotic expansions* 1956 (Dover Publications, Inc., New York).